Multiobjective Optimization of a Stent in a Fluid-Structure Context

Adel Blouza
Laboratoire Raphael Salem
Université de Rouen, France
adel.blouza@univ-rouen.fr

Laurent Dumas
Laboratoire J.L. Lions
Université Pierre et Marie Curie, France
laurent.dumas@upmc.fr

Ibrahima M'Baye
Laboratoire de Mathématiques
Université de Haute-Alsace, France
ibrahima.mbaye@uha.fr

ABSTRACT

A stent device is a permanent metallic implant currently used to prop open arteries blocked with atherosclerotic plaques. Many classes of stents are available and mainly differ by their design. Our purpose in this paper is to determine some optimal stent parameters to ensure a conforming blood flow through the stented artery. Coupling computational fluid dynamics with stochastic optimization based method is used to obtain the optimal parameters of a simplified stent. Our results point out that the obtained related stents overcome or at least reduce the risk of the late restenosis in stented segments.

Categories and Subject Descriptors

J.3 [**Computer Applications**]: Life and medical sciences

General Terms

Algorithms

Keywords

optimization, stent, fluid-structure interaction

1. INTRODUCTION

Cardiovascular diseases are the first cause of death in Europe. For two decades, they constitute an important subject of clinical investigations and academic studies. The well known stenosis pathology — reduction of the vascular lumen of an artery— affects the dynamics of the blood flowing through arteries and may even obturate them.

An appropriate procedure to eradicate this constriction is a balloon angioplasty, and/or a stent placement ([1], [3]). In the latter procedure, a stent is transported by a catheter, known as a stent delivery device, to the defective site in the artery and then expanded radially by the balloon to dilate the site (see Figure 1).

Though this method is commonly used by practitioners, the stent treatment is not a perfect solution and is often associated with complications such as restenosis. Indeed, numerous clinical studies describe the vessel damage during stent implantation and thereof the arterial wall growth over the wire mesh of the prothesis for about 20-30% of the patients who receive it.

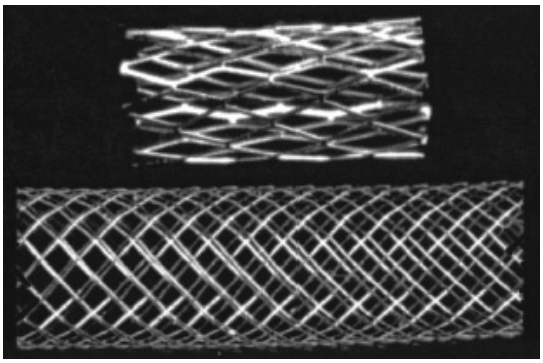

Figure 1: A balloon expandable stent.

To date, attempts have been made to treat the late restenosis by systemic administration of drugs. However these attempts have not been successful. Hence, current research is being shifted gradually to the local administration of various pharmaceutical agents at the site of an arterial injury resulting from angioplasty. Numerous attempts to develop stents with a local drug-distribution function have been made, most of which are variances of the so-called coated stent ([13]), a metal stent covered with a polymer envelope, containing anti-proliferative medicaments.

Many numerical simulations have been done, by following various approaches, to understand why restenosis occurs. Some authors have carefully studied the two-dimensional ([1], [2], [3], [4], [5]) or even three-dimensional ([14], [15]) blood flow behavior through stented arteries. Others have focused on the mechanical properties of the stent ([10]) or on chemical aspects of coated stents ([13]). In this last article, the authors have derived periodic and asymptotic coated stent models for the drug dose. They insist on the effect of the struts number and on the ratio between the area of the coated struts and the diseased segment of the artery on the distribution of the medicinal dose.

To the best of our knowledge, a multi-criteria optimization setting has never been considered to find the optimal geometric stent parameters.

We adopt, here, the fluid-structure approach to describe

GECCO'08, July 12–16, 2008, Atlanta, Georgia, USA.

the problem. We then couple equations with a stochastic optimization process in order to define optimal stent designs. More precisely, we are seeking with the best three geometric parameters of a simplified two-dimensional stent, namely the strut spacing l, the strut height h and the strut width w that could reduce blood stagnation and also fluid swirl. We will also see that these optimal parameters give us an optimal number of struts for a given target segment length. In our study, the blood flow is described by the two-dimensional steady Stokes equations on a deformed domain due to the fluid-structure interaction. To perform optimization, a multicriteria genetic algorithm is used.

The paper is organized as follows: in section 2, the numerical modelling of the flow through stented artery is presented and illustrated with three examples of stent designs. Section 3 is devoted to the description of the multiobjective optimization results for a large range of stent shapes. The last section gives some comments on the results of the present study.

2. NUMERICAL SIMULATION

2.1 Modelling of the fluid-stent interaction

In order to perform fast computations in view of the forthcoming optimization process, some simplifying hypotheses are made on the stent geometry and on the fluid flow. First, as is usually done by different authors ([1], [2]), the blood flow is assumed to be two-dimensional and the presence of the stent is modelled by the appearance in the arterial geometry of small periodic obstacles called struts. The corresponding fluid domain, is depicted on Figure 2. The stent

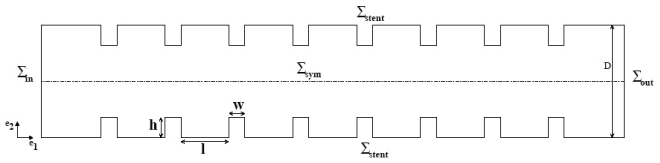

Figure 2: Simplified 2d-geometry of a stent and associated fluid domain.

shape is characterized by three different values: the strut spacing l, the strut height h and the strut width w.

Eight struts are observed to study the flow behavior inside the stent, here between the 4th and 5th strut where the effects of the boundary conditions enforced on Σ_{in} and Σ_{out} are attenuated.

The fluid is supposed to be viscous, incompressible and governed by the steady Stokes equations on the half fluid domain called Ω_F. In absence of any interaction with the stent structure, the velocity and pressure of the fluid, respectively denoted by $v = (v_1, v_2) : \Omega_F \to \mathbb{R}^2$ and $p : \Omega_F \to \mathbb{R}$, are solution of the following system of equations and boundary conditions:

$$\left\{ \begin{array}{rrcl} -\mu\Delta v + \nabla p &= 0 & \text{on} & \Omega_F \\ \text{div}(v) &= 0 & \text{on} & \Omega_F \\ v &= V_{in}(x_2)e_1 & \text{on} & \Sigma_{in} \\ v_2 = 0 \quad \text{and} \quad \dfrac{\partial v_1}{\partial x_2} &= 0 & \text{on} & \Sigma_{sym} \\ v &= 0 & \text{on} & \Sigma_{stent} \end{array} \right. \tag{1}$$

In these equations, μ and V_{in} respectively denote the fluid dynamic viscosity and the entrance velocity.

In order to take into account the interaction between the fluid and the structure, the stent is described by an elastic curved rod model. In this case, the fluid domain where the Stokes system (1) is solved, is no longer equal to Ω_F. Let us denote by $u : (0, L) \to \mathbb{R}$, the vertical deformation of the stent at position $x_1 \in (0, L)$. The previous system (1) is solved on a deformed domain called $\tilde{\Omega}_F$ and is coupled with the equations of the stent structure. In our case, these equations write in the following way:

$$\left\{ \begin{array}{rl} u^{(4)}(x_1) &= \frac{1}{d}\dfrac{\partial v_2}{\partial x_2}(x_1, u(x_1))\sqrt{1 + (u'(x_1))^2} \quad \text{on } (0, L) \\ u(0) &= u(L) = u'(0) = u'(L) = 0 \end{array} \right. \tag{2}$$

In the previous equation, the coefficient d is given by the relation $d = E\dfrac{W^3}{12(1-\alpha^2)}$ where W, E and α denote respectively the structure width, the structure Young modulus and the Poisson coefficient of the material.

2.2 Details of the numerical simulation

The solution of the coupled system of equations (1)-(2) is obtained by solving a fixed point problem with a BFGS method applied on a least square cost function (see [12] and [17] for more details on this method).

The corresponding algorithm is implemented with the help of a 2D finite element package FreeFem++, which is freely available [6]. For visualization, we use Medit, a free visualization sofware [7] .

A triangular mesh of the undeformed fluid domain Ω_F is created. It is made, approximately of 23000 triangles and 12000 nodes. An example of such mesh between two consecutive struts is given in Figure 3 (truncated mesh from the mesh of the domain Ω_F). For all the simulations done here, note that the artery diameter before deformation is taken equal to $D = 4$mm.

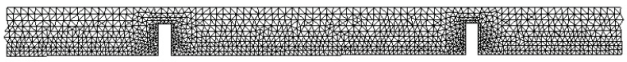

Figure 3: Mesh example of the undeformed half fluid domain Ω_F.

The ingoing fluid profile on Σ_{in} is supposed to be parabolic with a maximal value V_{max} on the symmetry axis Σ_{sym}. Two values of V_{max} are tested (namely 10 and 30 cm/s) corresponding to the extremal values of a real pulsatile blood flow.

The other characteristics of the fluid and the stent structure are given in Table 1.

fluid dynamic viscosity: μ	$0.035 g/cm.s$
Structure width: W	$0.01\,cm$
Young modulus: E	$110 \cdot 10^{10}\, g/cm \cdot s^2$
Poisson coefficient : α	0.33

Table 1: Fluid and stent structure data.

2.3 Qualitative behavior of the fluid flow

We first test the effect of the stent parameters (l, h, w) and the influence of the fluid-structure interaction on the flow characteristics. Three different examples are presented here corresponding to three different values of strut spacing l for a given strut height h and strut width w (see Table 2).

Case	l(mm)	h(mm)	w(mm)	l/h
1	2	0.25	0.08	8
2	0.75	0.25	0.08	3
3	0.25	0.25	0.08	1

Table 2: Three examples of stent parameters.

The results of the fluid-structure computation for the first case are presented on Figures 4 and 5. We also observe the stent deformation in Figure 4.

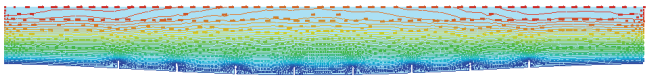

Figure 4: Case 1. Velocity streamlines and structure deformation, $V_{max} = 30cm/s$.

A zoom between the 4th and the 5th strut is presented on Figure 5. In this case, two counter rotating recirculation zones before and after each strut are clearly visible with a reattachment zone between them. A similar computation has been done without fluid structure interaction and the results point out the same flow behavior. However, on a quantitative viewpoint, there exists some differences for instance on the value of the wall shear stress (see the next subsection).

The results of the second and third cases are presented on Figure 6. For the second case, we observe that the flow is no longer reattached between the two vortices whereas only one recirculation zone is visible between two consecutive struts in the third case. Note that, as previously, the results with or without interaction (not illustrated here) are very similar on a qualitative viewpoint.

These results are coherent with previous observations made by other authors with the stent modelled as a rigid body ([1], [4], [5]).

In order to classify the different flow behaviors, an dimensionless value measuring the ratio between the strut distance and the strut height

$$r = \frac{l}{h}$$

is introduced. Depending on the values of l and h for a given strut width w, the following three cases between two consecutive struts can occur:

- for $r > r_u$: the flow is reattached during the whole cardiac cycle.
- for $r_u > r > r_l$: two recirculation zones without reattachement are visible during a part or the whole cardiac cycle.
- for $r_l > r$: only one recirculation zone is visible during a part or the whole cardiac cycle.

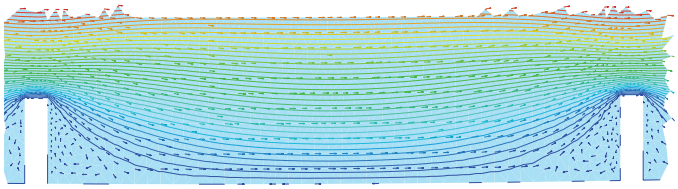

Figure 5: Two recirculation zones with reattachment (case 1).

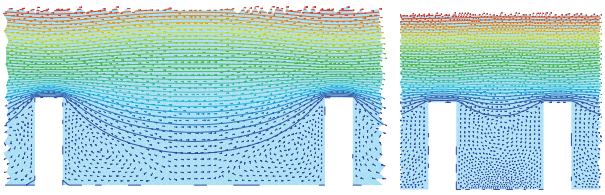

Figure 6: Two recirculation zones without reattachment (case 2, left) and one recirculation zone (case 3, right).

These results are summarized on Figure 7.

The accurate determination of the threshold values r_u and r_l is a difficult task. In [5], the value $r_u = 6$ is proposed. In this work, the value of r_u is slightly lower and ranges around 5.7 whereas the value of r_l is approximately equal to 2.

The present approach provide a more accurate design rule by seeking for the optimal stents in a large admissible domain with respect to two performance criteria described below.

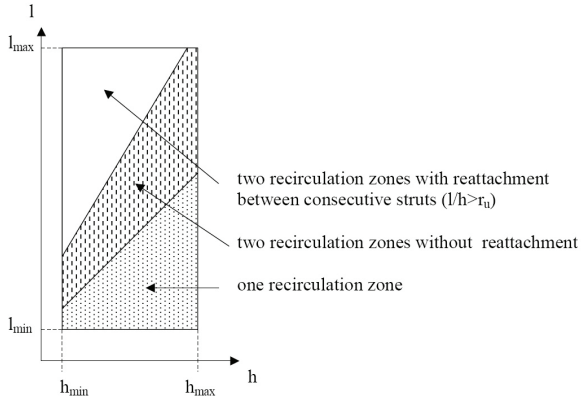

Figure 7: Qualitative behavior of the flow depending on l and h.

3. MULTIOBJECTIVE OPTIMIZATION

3.1 Definition of two performance criteria

In order to have a systematic and automatic approach designing a stent with the best characteristics, two perfor-

mances criteria are defined for a given stent, characterised here by its three parameters l, h and w.

The first performance criteria is the mean square wall shear stress between two consecutive struts, that is

$$J_1(l,h,w) = \frac{1}{\text{length}(\Gamma)} \sqrt{\int_\Gamma \left(\mu(\frac{\partial v_2}{\partial x_1} + \frac{\partial v_1}{\partial x_2}) \right)^2 d\gamma}$$

where Γ is the part of the stent boundary between the 4th and 5th strut (see Figure 8). As it has already been observed ([1], [5]), a stent associated with a higher value of J_1 will be preferred because it lowers the risk of the late restenosis by reducing the presence of blood stagnation.

Another performance criteria for a given stent is also considered here. It consists of a mean swirl value near the struts:

$$J_2(l,h,w) = \frac{1}{\text{area}(\omega)} \sqrt{\int_\omega \left(\frac{\partial v_2}{\partial x_1} - \frac{\partial v_1}{\partial x_2} \right)^2 dx_1 dx_2},$$

The integration domain ω has a rectangular shape (in absence of deformation) of base Γ and a constant height equal to $\frac{D}{6}$. As it has already been reported ([8]), a blood flow associated with a small value of J_2 is preferred.

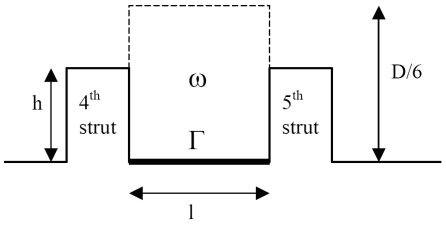

Figure 8: Definiton of the integration domains ω and Γ.

The performance values for the three stents studied in the previous section are given in Table 3 and Table 4.

The first striking observation is the large range of variations of both criteria depending on the configuration. The influence of the fluid structure interaction is also clearly visible even though it does not modify the respective order between the three cases.

For these three examples, the best stent design is the first one for both performance criteria, with or without fluid-structure interaction. However, note that a high wall shear stress value will not necessarily imply a low swirl value. Indeed, the first criteria is linked to the presence or not of large stagnation zones near the struts whereas the second rather measures the velocity streamline curvature due to the presence of struts. This observation will be checked by the multiple objective optimization presented below.

Cases	Shear stress (dynes/cm^2)	swirl (1/s)
1	$J_1 = 7.92$	$J_2 = 1673$
2	$J_1 = 2.46$	$J_2 = 3599$
3	$J_1 = 2.53$	$J_2 = 5393$

Table 3: Performance criteria for three examples of stents, with fluid-structure interaction.

Cases	Shear stress (dynes/cm^2)	swirl (1/s)
1	$J_1 = 13.11$	$J_2 = 2186$
2	$J_1 = 2.55$	$J_2 = 3624$
3	$J_1 = 2.56$	$J_2 = 6638$

Table 4: Performance criteria for three examples of stents, without fluid-structure interaction.

3.2 Details of the multiobjective optimization algorithm

In order to determine optimal stents with respect to the two performance criteria introduced above, a multiobjective optimization is performed with a genetic algorithm. This method is chosen here because it has already obtain, in many applicative fields, robust and global optimal solutions ([11], [16], [18]). Moreover, it is well adapted to determine a set of optimal solutions located on the Pareto front in the case of multioptimization problems. More precisely, the ϵ-multiobjective evolutionary algorithm, developed by K. Deb ([9]) and freely available at the site `http://www.iitk.ac.in/kangal/soft.htm`, is used for all the computations done here. It is based on the ϵ dominance principle that relaxes the classical dominance principle with a factor ϵ and also on the use of two co-evolving populations (an EA population and an archive population). A good diversity is ensured by allowing on the Pareto front only one solution in each hyper box.

The three stent design parameters l, h and w lie in a rather large domain, namely the following hypercube of $\mathbb{R}^3$:

$$(l,h,w) \in [0.02, 0.2] \times [0.01, 0.04] \times [0.007, 0.009] (\text{in cm})$$

In particular, it allows for the characteristic ratio $r = \frac{l}{h}$ allows to vary between 0.5 and 20.

A population of 100 individuals associated with 60 generations has been necessary to achieve the results presented below. Depending on the method used to compute the two cost functions, with or without fluid structure interaction, the total CPU time for an optimization process ranges from 2 hours to 20 hours on a Pentium 2Ghz PC.

3.3 Results

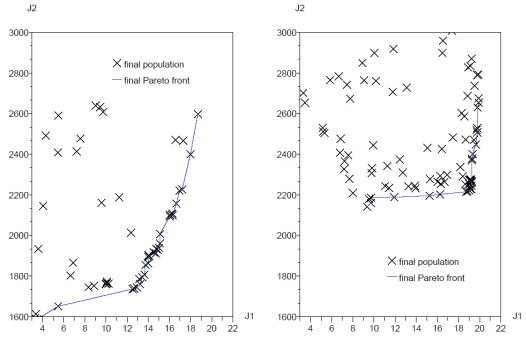

Figure 9: Multiobjective optimization: Pareto fronts of optimal stents (left: with fluid-structure interaction, right: without), $V_{max} = 30$cm/s.

The results of the multiobjective optimization algorithm are presented in Figures 9 and 10. The Pareto front, that is the set of optimal solutions with respect to the two performance criteria, the wall shear stress J_1 to maximize and the swirl J_2 to minimize, are depicted in Figure 9.

The values of l and h for all the optimal stents located on the Pareto front are represented in Figure 10. The corresponding value of w has not been depicted because it has been observed that this value has a minor influence on the two performance criteria. On this figure, the optimal stents associated to a high wall shear stress are located on one end of the curve whereas the other end corresponds to stents having rather a low swirl.

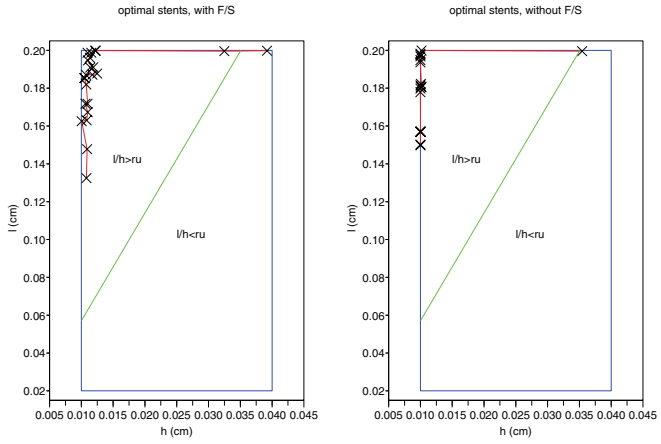

Figure 10: Optimal stent shapes depending on the model (left: with fluid-structure interaction, right: without).

From Figure 9 and Figure 10, one can also observe that the Pareto front is rather spread. It means that the chosen performance criteria are often conflicting. The interest of the Pareto front approach in this context is thus to allow the designer to choose the appropriate stent design, depending on which criteria to enhance.

Thus, an optimization process seems to bring a real improvement compared to a less systematic approach that is currently used for the design of stents.

The influence of the fluid-structure interaction that has also been investigated in this work, is clearly visible by comparing the two Pareto fronts on Figure 9. However, the corresponding stent shapes compared on Figure 10 are much closer, indicating that a pure fluid approach is sufficient at a first decision level.

Figure 10 gives the most important criteria to fulfill for designing optimal stents: in all cases, the ratio $r = l/h$ has to be chosen greater than r_u. As it has been observed in the previous qualitative observations on the fluid flow, it corresponds to a situation where the two recirculation areas before and after each strut are separated. Moreover, a higher ratio, that can be raised up to 20 in our study, is not always preferable as it can be observed on the stents depicted on Figure 10. Note also that the strut width w only plays a secondary role compared to l and h in the optimization process. It will thus be adjusted by the designer at its convenience.

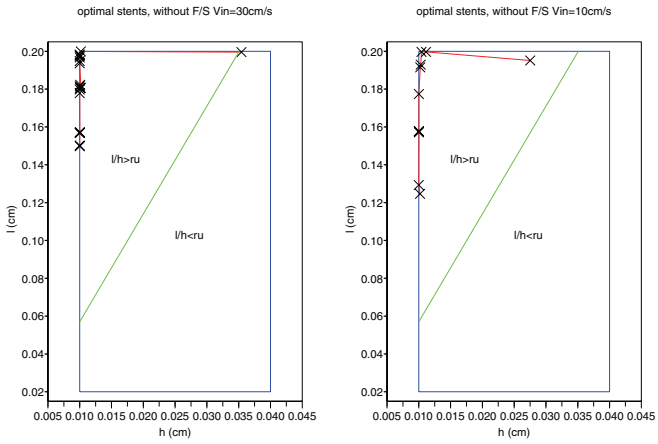

Figure 11: Optimal stent shapes depending on the initial velocity (left: $Vin = 30$m/s, right: $Vin = 10$m/s).

All the optimization results presented here are done with a maximal velocity value for the entrance profile equal to $30cm/s$. It is worth noticing that the obtained optimal stent shapes are nearly identical when taking the other extremal value of a real pulsatile flow, that is $10cm/s$ (see Figure 11), thus justifying a posteriori the steady flow hypothesis.

4. DISCUSSION

The purpose of this study is to evaluate the effects of varing stent design parameters on artery wall shear stress and on flow swirl around struts, using finite element analysis in fluid-structure context.

Let us recall that, in the case of blood stagnation between struts, the endothelial cells do not undergo usual shear. Their functioning is then disturbed, especially the production and release of chemical agents that inhibits the proliferation of smooth muscle cells. Furthermore, in the absence of shear, the probability of blood coagulation rises. The stent must thereby be designed to generate an appropriate shear at its interface with the blood flow.

From the study above, one can point out some remarks and comments. First, let us note that when the ratio $r = l/h$ is decreased below a critical value r_u, both performance criteria are degenerating because of the topological change of the flow between two consecutive struts.

Another important observation coming from this work is the relative independence on the design results of some simplificatory hypotheses that can be made during the modelling phase, such as the steady flow hypothesis or the absence of fluid-structure interaction.

Finally, as we know, the number of struts for a coated stent is an important parameter for the efficiency of the treatment with drug covering stents. One can naively think that the best way is to use a stent with high number of struts for a drug-distribution function, even though the de-

ployment of such a stent in the artery can be seriously invasive.

Thanks to our study, at a given h and w, when we choose the optimum strut spacing l such that the ratio r fits with the appropriate values of the cost functions, we implicitly give the best number of struts for a given stent length.

Conclusion

The current results using a 2d computational fluid-structure modelling and a multiobjective optimization loop indicate that there exist some important rules to fulfill in order to design appropriate stents which may avoid or at least reduce restenosis. The main rule can be summarised by saying that the characteristic ratio "strut spacing over strut height" shall be above the critical value $r_u = 5.7$ to ensure a sufficiently high wall shear stress while maintaining a low level of flow swirl. When this ratio is decreased, both performance criteria are degenerating because of the topological change of the flow between two consecutive struts.

Acknowledgments

The authors wish to thank Marc Thiriet for fruitful discussion on this subject.

5. REFERENCES

[1] J. L. Berry, A. Santamarina, J. E. Moore Jr., S. Roychowdhury, and W. D. Routh, Experimental and Computational Flow Evaluation of Coronary Stents, Annals of Biomedical Engineering, Vol 28, pp. 386-398, 2000.

[2] A. I. Barakat, and E. T. Cheng, Numerical Simulation of Fluid Mechanical Distrurbance Induced by Intravascular Stents, Proceedings of ICMMB-11: International Conference on Mechanics in Medecine and Biology, 2000.

[3] S. Sukavaneshvar, G. M. Rosa and K. A. Solen, Enhancement of Stent-Induced Thromboembolism by Residual Stenoses: Contribution of Hemodynamics. Annals of Biomedical Enginneering, Vol. 28. pp. 182-193, 2000.

[4] A. O. Frank, P. W. Walsh and J. E. Moore Jr, Computational Fluid Dynamics and Stent Design. Artificial Organs, 26(7): 614-621, Blackwell Publishing, Inc., 2002.

[5] J. E. Moore Jr, and J. L. Berry, Fluid and Solid Mechanical Implications of Vascular Stenting, Annals of Biomedical Engineering, Vol 30, pp. 498–508, 2002.

[6] F. Hecht, O. Pironneau. A finite element Software for PDE: FreeFem++ (www.freefem.org).

[7] P. Frey. Medit, a Mesh visualization Software (www.ann.jussieu.fr/frey/logiciels/medit.html)

[8] A. Quarteroni and G.Rozza, Optimal Control and Shape Optimization in Aorto-Coronaric Bypass Anastomoses, Mathematical Models and Methods in Applied Sciences, Vol.13, 2003.

[9] K. Deb, M. Mohan and S. Mishra, A Fast Multiobjective Evolutionary Algorithm for Finding Well-Spread Pareto-Optimal Solutions. KanGAL Report Number 2003002, 2003.

[10] T. A. Guimaraes , M. A.V. Duarte and S. A. G. Oliveira, Topology Optimization of the Stent Cells Plane Model With Maximum Hardening and Flexibility, Inverse Problems, Design Theory and Optimization Symposia. Rio de Janeiro, ABCM, p. 1-8, 2004.

[11] L. Dumas, V. Herbert and F. Muyl, Comparison of Global Optimization Methods for Drag Reduction in the Automotive Industry, Lecture Notes in Computer Science 3483, p. 948-957, 2005

[12] C. Murea, The BFGS Algorithm for Nonlinear Least Squares Problem arising from Blood Flow in Arteries. Comput. Math. Appl., Vol. 49, p. 171-186, 2005.

[13] M. C. Delfour, A. Garon and V. Longo, Modeling and Design of Coated Stents to Optimize the Effect of the Dose, Siam Journal on Applied Mathematics, 65(3), p. 858-881, 2005.

[14] N. Benard, Analyse de l'écoulement physiologique dans un stent coronarien: application à la caractérisation des zones de resténose pariétale, PhD thesis, Université de Poitiers, 2005.

[15] J.F. LaDisa, Jr., L.E. Olson, D.A. Hettrick, D.C. Warltier, J.R. Kersten and P.S. Pagel, Axial stent strut angle influences wall shear stress after stent implantation: analysis using 3D computational fluid dynamics models of stent foreshortening. Biomedical Engineering Online, 4:59, 2005

[16] L. Dumas, B. Ivorra, B. Mohammadi, P. Redont and O. Durand, Semi deterministic vs Genetic Algorithms for Global Optimization of Multichannel Optical Filters, to appear in International Journal of Computational Science and Engineering, 2006.

[17] I. MBaye, Etude mathématique et numérique de quelques problèmes de couplage fluide-structure , PhD thesis, Université de Mulhouse, 2006.

[18] L. Dumas, L. El Alaoui, How Genetic Algorithms can improve a pacemaker efficiency, proceedings of GECCO 2007, p. 2681-2686, 2007.